Ceramics International 42 (2016) 17398–17404

Contents lists available at ScienceDirect

Ceramics International

journal homepage: www.elsevier.com/locate/ceramint

Effect of heating rate on the shrinkage and microstructure of liquid phase sintered SiC ceramics

S. Ribeiro [a,*], L.A. Gênova [b], G.C. Ribeiro [a], M.R. Oliveira [a], A.H.A. Bressiani [b]

[a] University of São Paulo (USP), Lorena School of Engineering (EEL), Department of Materials Engineering (DEMAR), Estrada Santa Lucrecia s/no, Bairro Mondezir, CEP 12600-970 Lorena, SP, Brazil
[b] Institute for Energy and Nuclear Research (IPEN), Brazil

ARTICLE INFO

Article history:
Received 29 March 2016
Received in revised form
4 July 2016
Accepted 6 August 2016
Available online 6 August 2016

Keywords:
D.SiC
Dilatometry
Shrinkage
Heating rate

ABSTRACT

This paper describes a study of shrinkage behavior in the liquid phase sintering of silicon carbide, SiC, using eutectic mixtures of $Al_2O_3+Dy_2O_3$ and $Al_2O_3+Yb_2O_3$ as liquid-forming additives. A volume fraction 10% of these mixtures was added to the SiC and homogenized in an attrition mill. Sintering was performed in a horizontal dilatometer at 1800 °C for 60 min, applying heating rates of 10, 20 and 30 °C/min. The results indicate that these heating rates affected neither shrinkage nor microstructure, from the standpoint of the complete sintering cycle. However, significant differences occurred during the non-isothermal sintering stage, leading to very different shrinkage results as a function of the heating rate. Higher heating rates produced lower shrinkage, and the work of final shrinkage occurred during the isothermal stage.

1. Introduction

Silicon carbide, SiC, ceramics are still one of the most widely studied ceramics, as can be seen from high visibility bibliographic databases. This is obviously due to their properties, and hence, their broad range of applications. The main properties of SiC ceramics include: high modulus of rupture and of elasticity, high hardness and wear resistance, good corrosion resistance and thermal conductivity, as well as low density and thermal expansion coefficient. Their numerous applications include: diesel engine components, gas turbines, industrial heat exchangers, high temperature energy conversion systems, fusion reactor parts, hot gas filters, ring gaskets, semiconductor processing equipment, tribological applications in different atmospheres, medical implants and optical mirrors [1–15].

SiC sintering can be performed via solid or liquid phase. Solid phase sintering requires the addition of substances that alter the surface energy of SiC, enabling it to densify. SiC is difficult to densify even when using additives and high temperatures, because it is a chemical substance with predominantly covalent bonds and a low self-diffusion coefficient, which hinder the mass transport mechanisms responsible for its densification [10,11,14]. The additives traditionally used in the solid phase sintering of SiC are carbon, boron and aluminum [1,2,7–9,14,16].

The most common procedure to produce SiC ceramics is via liquid phase sintering. The presence of a liquid phase accelerates mass transport, and reduces the temperature and sintering time, resulting in a fine-grained and more homogeneous microstructure with better mechanical performance, particularly fracture toughness. The final microstructure depends on the proportions of α-β-SiC, the quantities and types of additives, and the sintering time and temperature [11,17,18]. Liquid phase sintering initially yields a compact composed of the base material and the liquid-forming additive. The most commonly used additives are mixtures of Al_2O_3-Y_2O_3, Al_2O_3-La_2O_3, and more recently, Al_2O_3-Yb_2O_3 and Al_2O_3-Dy_2O_3. The liquid formed by the rare earth oxide additives may show slight differences, because albeit similar, rare earths may exhibit different behaviors according to their atomic radii [17,19,20]. Our expectation was that the structure would not undergo significant changes, since previous works report only minor differences in response to various additives containing rare earths [19].

Soon after heating begins the compact expands slightly, at which point the sintering mechanisms are set in motion, namely: evaporation-condensation and surface diffusion, which cause little shrinkage. As the temperature increases, the additive, or additive mixture, melts and forms a liquid that should wet the base material, causing the particles to approach each other and to become rearranged, which leads to high shrinkage rates [21]. When this occurs, the base material should dissolve in the liquid, saturating this liquid and precipitating elsewhere in the system. These last two, i.e., saturation and precipitation, are the most important mechanisms that trigger the greatest shrinkage of the compact in

* Corresponding author.
E-mail address: sebastiao@demar.eel.usp.br (S. Ribeiro).

http://dx.doi.org/10.1016/j.ceramint.2016.08.039
0272-8842/

a relatively short time [22].

Wetting is a highly significant phenomenon in the liquid phase sintering process. It reflects the extent to which a liquid can adhere to or spread over a solid surface. Several studies have focused on determining the contact angle of various additives in SiC ceramics, aiming to apply them in the liquid phase sintering of this important ceramic material [6–8,10–15,17,23–27]. Experimental tests have shown that mixtures of Al_2O_3 and Dy_2O_3 or Yb_2O_3 produce contact angles lower than 20°, i.e., they are considered optimal wetting additives for SiC [26].

At the isotherm, particularly close to its end, the microstructure coalesces by increasing the average grain size, leading to microstructural coarsening of the ceramic [5]. At this stage, grain growth prevails over shrinkage, and hence, over densification.

Ceramics can be sintered in a dilatometer, for a single sample yields various types of information about the thermal behavior of the material throughout the sintering cycle (heating, isotherm, and cooling). Based on this information, curves can be drawn to represent the sample's dimensional variation over time or temperature, with a slight expansion at the onset, but with significant shrinkage, especially close to the sintering hold temperature. The curves reported in the literature represent shrinkage or density vs. temperature or time [21,28–38]. Although density is a very important parameter of sintering, these curves are often obtained erroneously from shrinkage data, for example, considering theoretical density using the rule of mixtures for systems that react to form new phases, isotropic thermal expansion, among others [30–36,38]. Thus, experimental results obtained in a dilatometer are often represented in the form of shrinkage and not of density [21,28,29,37].

A very important sintering parameter is the heating rate, whose influence on density and other properties of sintered materials and has been discuss by several authors [21,30–32,34,36–38]. Shrinkage behavior, as well as the effect of heating rate on densification, have aroused much controversy [21,39]. Reports in the literature indicate that the heating rates adopted for conventional sintering in a dilatometer range from 2 to 100 °C/min [36–43]. These values can be much higher in fast sintering, and their influence is much more pronounced [44,45].

Samples sintered at the lowest heating rate shrinks more than at the highest heating rate, which can be explained by the longer overall time the sample remains inside the furnace [21,38]. It has also been reported that lower heating rates lead to lower shrinkage onset temperatures, while higher heating rates produce lower shrinkage at the end of the heating stage [41–43].

Compacts produced from mixtures of SiC, SiO_2, Al_2O_3 and Y_2O_3, with various additive compositions, were sintered in a dilatometer, and the final shrinkage was found to be dependent on the composition, while shrinkage rates and maximum shrinkage temperatures were dependent on the heating rate [46]. In this work, as in most of the reports found in the literature, the complete sintering cycle was evaluated, without evaluating shrinkage during the non-isothermal heating [21,28–38,46].

The main purpose of this work was to study the effect of heating rate on the shrinkage and microstructure of SiC ceramics doped with mixtures of $Al_2O_3+Dy_2O_3$ and $Al_2O_3+Yb_2O_3$.

2. Experimental

The SiC samples with additives were prepared using the following materials: silicon carbide – SiC Grade BF-12 supplied by Hermann C. Starck (HCST); alumina oxide – Al_20_3, 99.99% purity, from Baikalox; ytterbium oxide – Yb_2O_3, 99.9% purity, from ABCR GmbH & Co; dysprosium oxide – Dy_2O_3, 99.99% purity, from ABCR GmbH & Co.; and isopropyl alcohol – $CH_3CHOHCH_3$ from Synth P.A. ACS.

Table 1
Composition of the SiC and additive mixtures (in weight).

Powder mixtures	Code of mixture	Components (g)			
		SiC	Al_2O_3	Yb_2O_3	Dy_2O_3
SiC + 10%vol.($Al_2O_3+Yb_2O_3$)	SiCYb	120	12.76	9.39	0.0
SiC + 10%vol.($Al_2O_3+Dy_2O_3$)	SiCDy	120	12.10	0.0	8.45

Two mixtures were prepared: one with SiC +10% vol. ($Al_2O_3+Dy_2O_3$) and the other with SiC +10% vol. ($Al_2O_3+Yb_2O_3$), with SiC (the base material) corresponding to 90% of the volume of the mixture and the additives representing 10%. The additives were used in their respective eutectic compositions. Table 1 describes the quantities of these materials used.

The powders listed in Table 1 were weighted and then mixed in an attrition mill at 600 rpm for 6 h, in isopropyl alcohol medium. After mixing, the slurry was dried under vacuum in a rotary evaporator, at 90 °C. After drying, the powders were deagglomerated in a Tyler 40 mesh sieve and isostatically pressed under 200 MPa, resulting in cylinders with a diameter of 6 mm and length of 10 mm.

The cylindrical samples were then sintered in a NETZSCH DIL402E/7 horizontal dilatometer operating under the following conditions: sintering hold temperature of 1800 °C, for 60 min, at heating rates of 10, 20 and 30 °C/min, under argon flow. The data from the dilatometer were used to prepare shrinkage vs. temperature and shrinkage vs. time curves using Origin 6 software.

The microstructural analysis was performed in a LEO 1450 VP scanning electron microscope (SEM), operating in secondary electron imaging mode, at an accelerating voltage of 20 kV and current of 3.2 mA. The samples were fractured at a constant displacement rate and coated with a gold thin film. To measure the grain size, the samples were sanded, polished, etched with borax, and their images recorded for a grain count, which was done using the intercept method [31,47].

3. Results and discussion

Fig. 1 illustrates the shrinkage vs. temperature curves of the SiCDy and SiCYb mixtures sintered at 1800 °C, using heating rates of 10, 20 and 30 °C/min, in a complete sintering cycle. Note that for the SiCDy mixture, curve (u), the 10 °C /min heating rate was the most favorable for total shrinkage, although the benefit was only minor, which was not the case for the SiCYb mixture. This may have been due to a slight difference in properties between the two liquids formed by the Al_2O_3-Dy_2O_3 and Al_2O_3-Yb_2O_3 oxides. One of the factors that can cause this difference is the ionic radius. The ionic radius of Dy is 91.2 pm and that of Yb is 86.8 pm [20]. An earlier study also found similar slight differences between other measured properties of the mixtures [19]. In general, based on an evaluation of the complete sintering cycle, it can be concluded that the heating rates did not significantly influence the behavior of the SiCDy and SiCYb mixtures.

The geometric aspect and numerical values are very similar, as can be observed in the (t), (u), (v), (x), (z) and (y) curves, including overlaps.

In Fig. 1(a) and (b), up to about 1200 °C and 1250 °C, respectively, note the slight increase in the original length of the sample, which is due to the natural expansion of the compact. In Fig. 1 (a) and (b), respectively, note the slight shrinkage occurring at temperatures of up to approximately 1660 and 1690 °C, which can be attributed to a primary particle rearrangement of SiC and

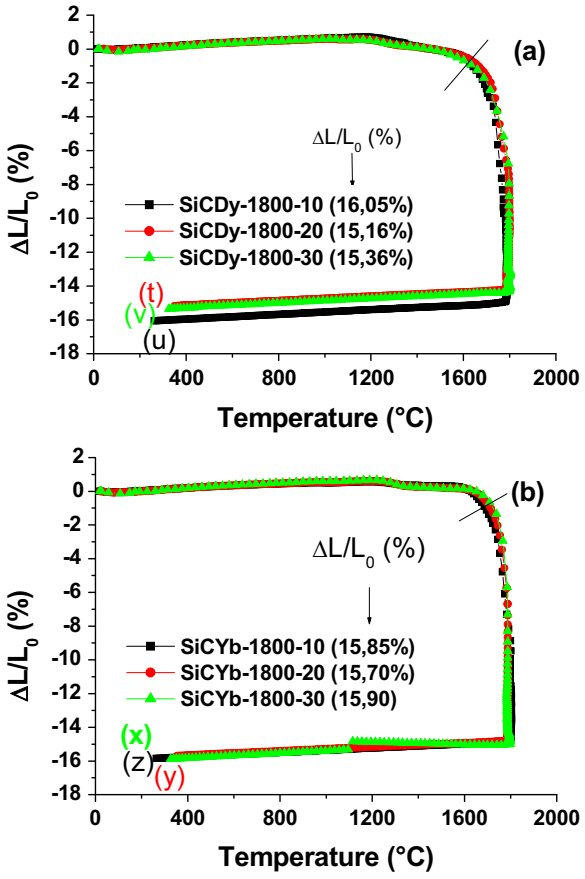

Fig. 1. Behavior of the SiCDy (a) and SiCYb (b) samples sintered for 1 h at 1800 °C at heating rates of 10 °C/min (u and z curves), 20 °C/min (t and y curves), and 30 °C/min (v and x curves): complete sintering cycle. The values in parentheses indicate the linear shrinkage at each heating rate.

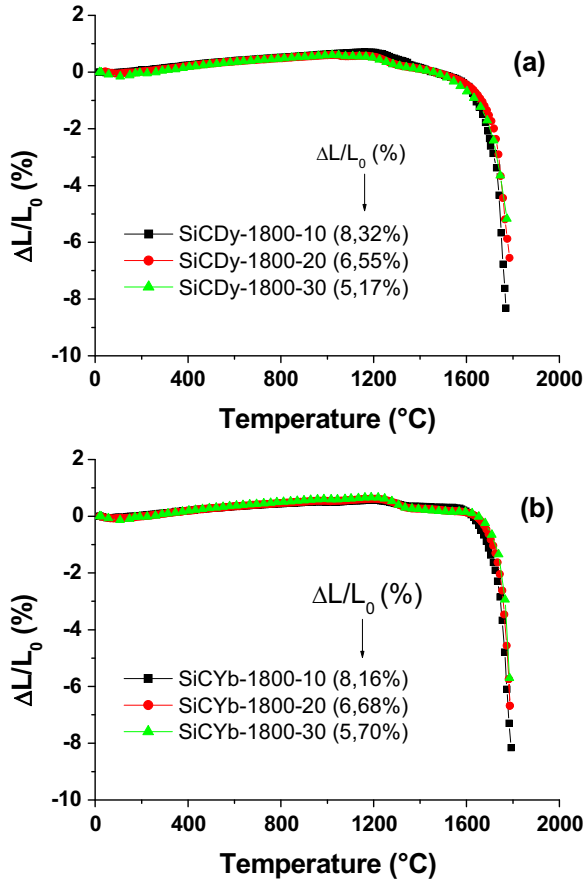

Fig. 2. Behavior of the dilatometric curves of the SiCDy (a) and SiCYb (b) mixtures during the heating stage, at heating rates of 10, 20 and 30 °C/min.

additives. Liquid begins to form slightly above these temperatures, which spreads around the SiC particles and causes them to dissolve and reprecipitate, producing high shrinkage rates in all cases, mixture and heating rate. This information is based on a previous study of eutectic mixtures of Al_2O_3-Dy_2O_3 and Al_2O_3-Yb_2O_3 oxides [26]. In the cited study [26], the melting temperatures of the individual oxide mixtures were found to be slightly higher, i.e., 1825 °C for Al_2O_3-Dy_2O_3 and 1850 °C for Al_2O_3-Yb_2O_3, than those observed in the mixtures with SiC. This presumably indicates that SiC interacts with the additives, forming a liquid containing SiC and the components of the mixtures. However, it is currently impossible to confirm this hypothesis, because there is no ternary phase diagram for SiC-Al_2O_3-Dy_2O_3 and SiC-Al_2O_3-Yb_2O_3, but this may be a subject for future research.

The behavior and discussion pertaining to Fig. 1 is quite common in publications involving sintering in a dilatometer, i.e., the complete sintering cycle, where what occurs in intermediate steps, e.g., during heating, cannot be verified. Therefore, in this study, we evaluated the behavior of the two mixtures at the three heating rates, whose results are indicated the curves in Fig. 2. This figure shows the shrinkage vs. temperature curve only during the heating step of the two mixtures at the three heating rates.

The influence of the heating rate on shrinkage in this sintering stage is clearly visible. The lowest heating rate results in higher shrinkage, which is due to the longer time the sample remains in the furnace to reach the isotherm temperature.

Table 2 lists the shrinkage in the different sintering stages. These values were determined based on the following criteria: the maximum or total shrinkage shown in Fig. 1, curves and points (t), (u), (v), (x), (z) and (y) (see the respective legends of Fig. 1(a) and (b)) were used; for shrinkage during heating stage, we used the shrinkage indicated in the legends of Fig. 2(a) and (b) divided by total shrinkage to find the percentage values. For example, SiCDy heated at 10 °C/min: $(0.0832/0.1605) \times 100 = 51.83\%$. This value indicates that 51.83% of the sample's linear shrinkage occurred during heating stage. Curves identical to the aforementioned ones were prepared for the isothermal sintering (threshold) and cooling step, and were calculated in the same way.

Table 2
Shrinkage observed in the heating, isothermal and cooling stages of sintering.

Characteristics evaluated	Mixture /heating rate (°C/min)					
	SiCDy			**SiCYb**		
	10	20	30	10	20	30
Shrinkage during heating stage (%)	51.83	43.15	34.06	51.48	42.09	35.85
Shrinkage at the sintering hold temperature (isothermal) (%)	41.12	50.46	60.41	41.89	51.17	58.49
Shrinkage during cooling (%)	6.96	6.39	6.72	6.55	5.80	5.66

Table 2 clearly indicates that the two mixtures behaved very similarly. Note that the heating rate strongly influenced the shrinkage in each analyzed stage. The results obtained in the heating stage of the SiCDy mixture show variations of 51.83%, 43.15% and 34.06% at the heating rates of 10 °C, 20 °C and 30 °C/min, respectively. The SiCYb mixture showed the same behavior.

Shrinkage at the sintering hold temperature increased with the heating rate, which is very clear, since shrinkage at the threshold

adjusts over time, leading to values very close to the final shrinkage.

In studies reported in the literature, shrinkage during cooling is disregarded, possibly because of the belief that dimensional variations no longer occur in this stage. However, this is incorrect, because considerable shrinkage still occurs, with values ranging

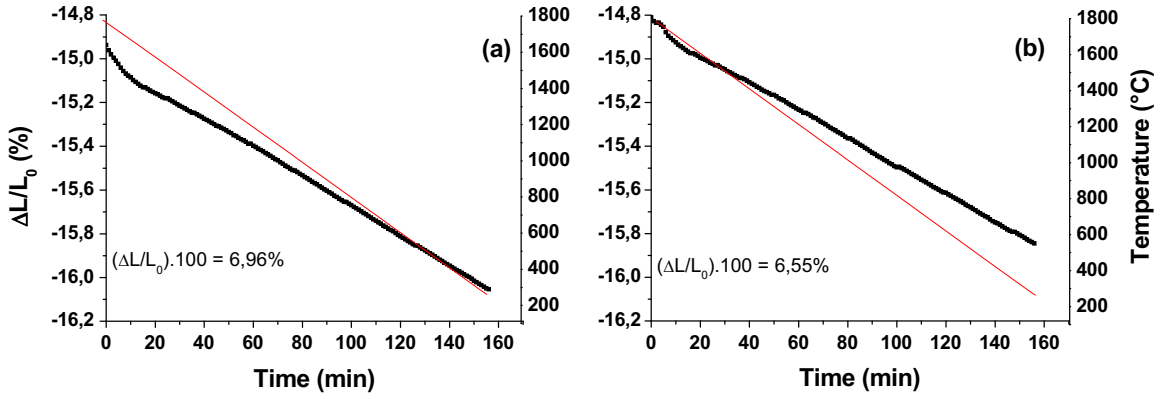

Fig. 3. Effect of the cooling stage on the shrinkage of SiCDy (a) and SiCYb (b) samples.

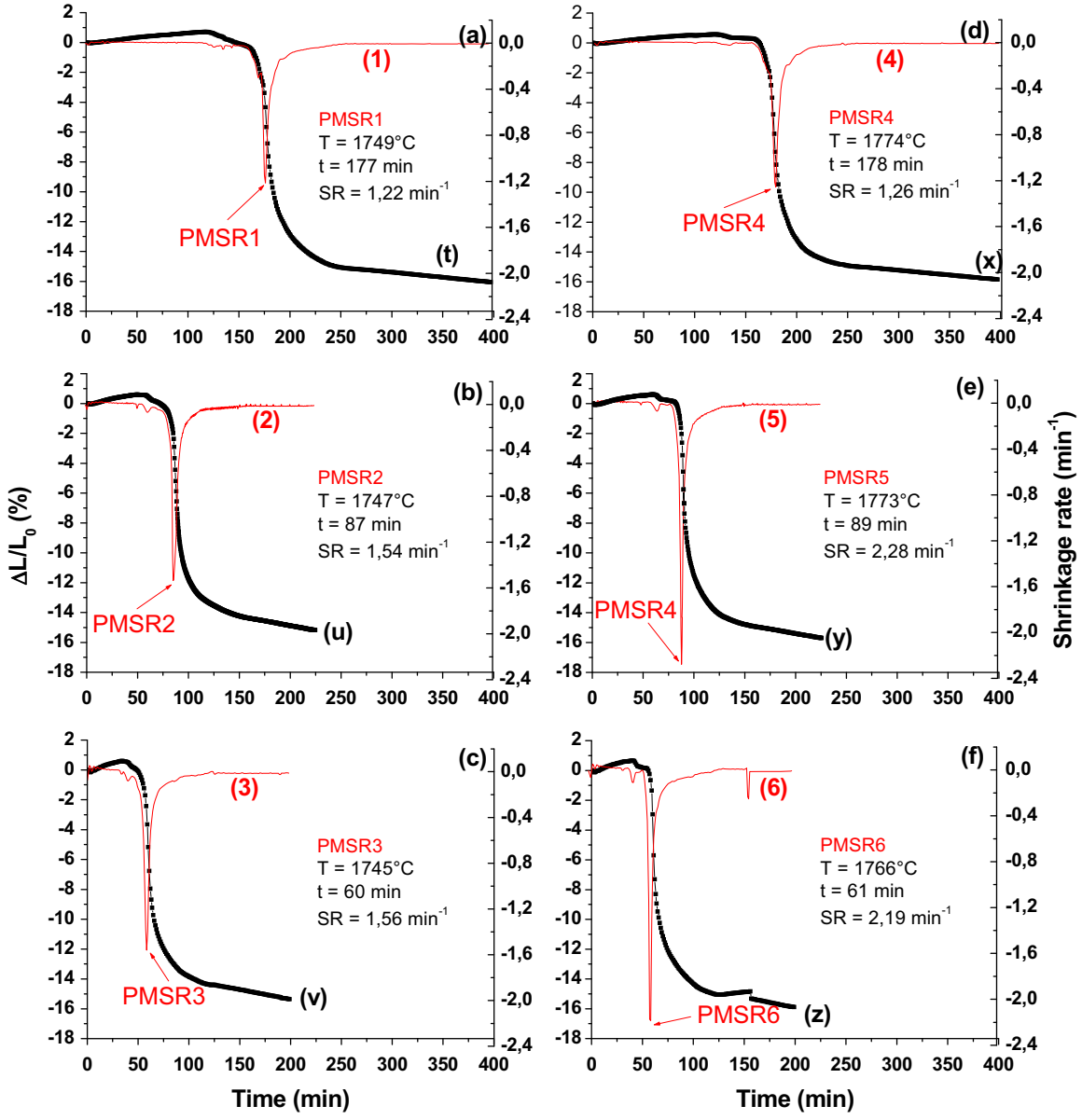

Fig. 4. Dilatometric curves of the SiCDy (a) , (b) and (c) and SiCYb (d), (e) and (f) mixtures sintered at 1800 °C, applying heating rates of 10 °C/min (a and d), 20 °C (b and e) and 30 °C/min (c and f). PMSR=Point of Maximum Shrinkage Rate; T=Temperature of PMRS, t=time of PMSR, and SR=shrinkage rate at the PMSR.

from 5.66 to 6.96%.

The graphs in Fig. 3, chosen randomly from among the ones prepared in this work, show the samples' shrinkage behavior during the cooling stage. Note that the shrinkage rate at the beginning of cooling is slightly higher than after longer times. This is physically consistent. Table 2 lists the values of linear shrinkage of all samples in the cooling stage.

Fig. 4 shows the shrinkage vs. time curves (curves t, u, v, x, y, z) and curves 1–6, which were produced by derivation of the shrinkage vs. time curves. The curves accurately indicate the temperatures corresponding to the onset of shrinkage and the moment when the shrinkage rate was at its highest, i.e., the Point of Maximum Shrinkage Rate (PMSR). The derived curves clearly illustrate successive changes in behavior, which are often not easily distinguishable in shrinkage vs. time curves. For example, in curves 1 and 4, note that at a heating rate of 10 °C/min, low-intensity events occur in the time between 120 and 150 min. At heating rates of 20–30 °C/min, these events become more significant between 30 and 50 min in both mixtures. It is believed that, at these points, mechanisms are triggered that cause slight shrinkage, for example, particle rearrangement followed by incipient solid state sintering, before the liquid is formed.

With the formation of liquid, the interparticle bonds break and shrinkage occurs very rapidly, as indicated by the point of maximum shrinkage rate, PMSR [21].

The derived curves 1-6 clearly indicate when and at what temperatures the highest shrinkage rates occur. These curves indicate that there are differences in the values of PMSR as a

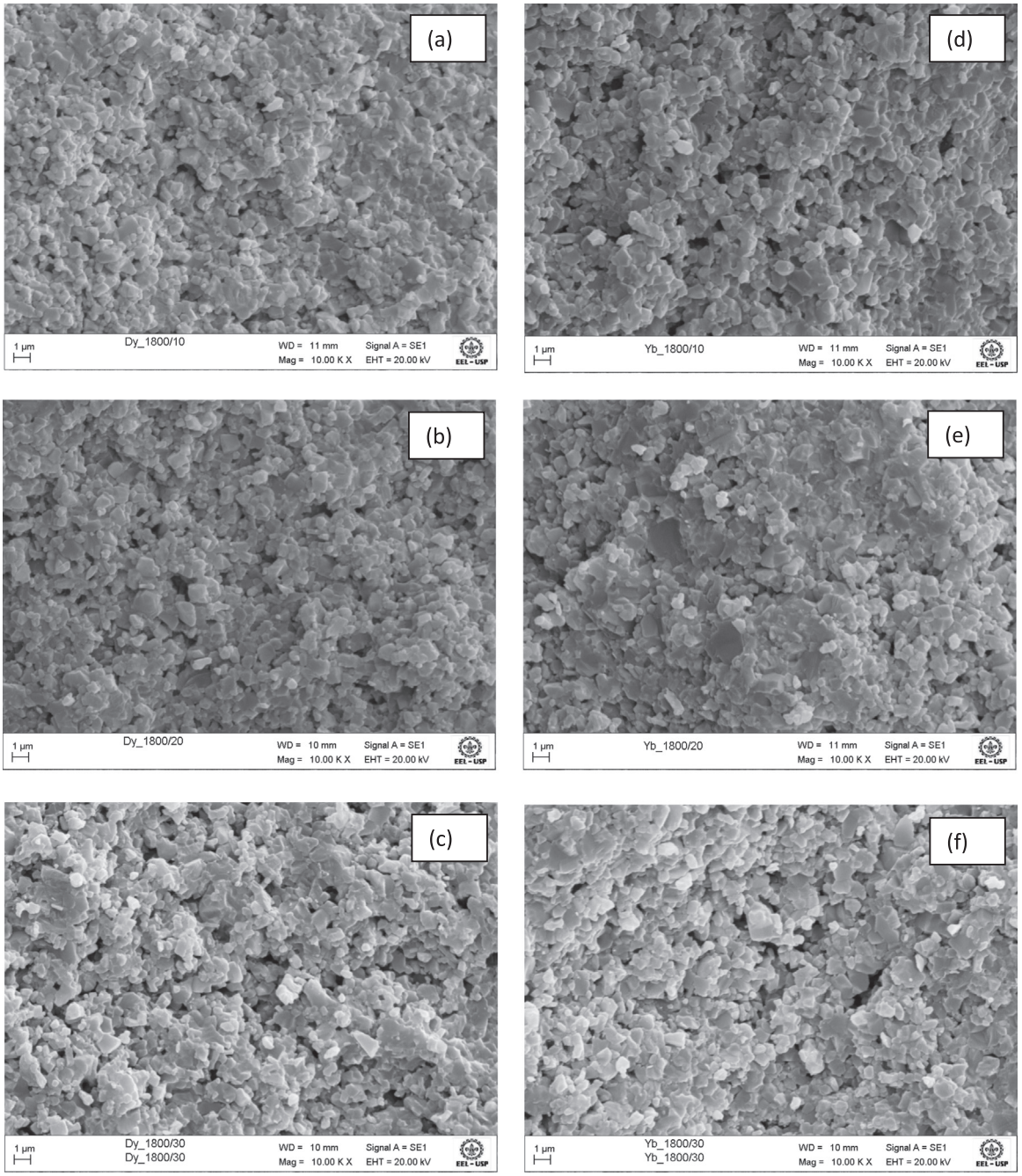

Fig. 5. SEM micrographs of the fracture surfaces of samples sintered for 1 h at 1800 °C in a dilatometer: (a, b, c) SiCDy mixtures, and (d, e, f) SiCYb mixtures, at heating rates of: (a, d) 10 °C/min; (b, e) 20 °C/min; and (c, f) 30 °C/min.

Table 3
Mean grain size of SiCDy and SiCYb mixtures sintered at 1800 °C, at heating rates of 10, 20 and 30 °C/min.

Mixture	Heating rate (°C/min)/grain size (μm)		
	10	20	30
SiCDy	0.77 ± 0.15	0.69 ± 0.09	0.63 ± 0.10
SiCYb	0.85 ± 0.13	0.69 ± 0.08	0.68 ± 0.12

function of the heating rate and composition. The values of temperature (T), time (t) and shrinkage rate (SR) are indicated in the captions of their respective curves. The difference in SR is negligible in curves 1 and 4, i.e., 1.22 and 1.26 $s^{-1,}$ respectively. However, a comparison of curve 1 against curves 2 and 3 reveals a slight increase in the PMSR, 1.54 and 1.56 $s^{-1,}$ respectively. The highest variations are in curves 5 and 6 of the SiCYb mixture, whose PMSR showed an increase of over 50%. This can be explained by the very fast formation of liquid, which did not allow enough time for the dissolution of SiC particles, which in the previous cases probably dissolved, and this less viscous liquid led to rapid particle rearrangement, causing very rapid shrinkage soon after its formation. Studies have shown that higher heating rates also cause higher maximum shrinkage rates [21,43].

The areas of the peaks correspond exactly to the duration of the events, i.e., the longer and wider, the greater the period of occurrence of the formation of the liquid, wetting and solution-precipitation. Higher heating rates produced wider curves.

As can be seen in the captions of the graph in Fig. 4, the temperatures at which the highest shrinkage rates occur are practically the same ones for the same mixture. Although they are slightly lower for the SiCDy samples than for the SiCYb samples, the two mixtures of additives show little difference in terms of thermal behavior. It can also be seen that, in all the cases, the PMSR occurs at temperatures below the threshold temperature, i.e., 1800 °C.

An important point to mention is the drawing up and study of the shrinkage vs. temperature curves of the heating stage, since the literature usually shows dilatometric curves corresponding only to the complete sintering cycle. In this study, the importance of the dilatometric curves in the heating stage was the revelation that the heating rate is very significant for this step and is thus able to provide more in-depth details for the preparation of sintering cycles. The differences found in the partial curves are eliminated, or disregarded, when the curves of the complete sintering cycle are evaluated.

Fig. 5 shows micrographs of the samples of SiCDy and SiCYb mixtures sintered at 1800 °C, applying heating rates of 10 °C, 20 °C and 30 °C/min.

An analysis of the micrographs indicates that the overall microstructure of the six samples is very similar in terms of homogeneity, morphology, porosity, grain size and distribution. These properties are typical of liquid phase sintered SiC ceramics, when liquid-generating additives with low contact angles are used [10,11,19]. The microstructure is essentially composed of relatively small, uniformly distributed plate-like grains. These micrographs are similar to those found in reference [19].

In this case, the influence of the heating rate on grain growth can be considered negligible. Table 3 lists the measured grain sizes of the two mixtures at the three heating rates.

The results for both the mixtures indicate that the grain size tends to decrease as the heating rate increases. These results are coherent, given that the residence time of the material under heating at lower heating rates is longer, thus resulting in larger grain size [5].

4. Conclusions

The heating rate plays an important role in shrinkage during the heating period, but may be negligible in the complete sintering cycle.

The heating rate does not significantly influence the sintering behavior of SiC in the complete cycle, contrary to long-standing principles of ceramic processing.

The highest shrinkage rates in both mixtures at the three heating rates occurred at temperatures below their respective sintering thresholds, indicating that a good part of the shrinkage occurs during the heating stage, and this can be used to optimize the liquid phase sintering of ceramics.

Dilatometry is a good tool to understand and predict the behavior of all the sintering stages of ceramics.

The behavior of the two rare earth oxides used as additives in the liquid phase sintering of SiC was similar.

From a technical standpoint, the rare earth oxides Dy_2O_3 and Yb_2O_3 are excellent candidates in the composition of mixtures with Al_2O_3 for liquid phase sintering of SiC ceramics.

Acknowledgments

The authors gratefully acknowledge the Brazilian research funding agencies FAPESP (São Paulo Research Foundation), process nos. 2010/51925-6 and 2013/08032-9, and CNPq (National Council for Scientific and Technological Development), process nos. 303061/2009-0 and 307432/2013-0, for awarding Research Productivity grants.

References

[1] J. Zhang, D. Jiang, Q. Lin, Z. Chen, Z. Huang, Properties of silicon carbide ceramics from gelcasting and pressureless sintering, Mater. Des. 65 (2015) 12–16.
[2] N.A. Nasiri, E. Saiz, F. Giuliani, L.J. Vandeperre, Effect of microstructure and slow crack growth on lifetime prediction of monolitic silicon carbide, Mater. Sci. Eng. A627 (2015) 290–295.
[3] S. Lafon-Placette, K. Delbé, J. Denape, M. Ferrato, Tribological charcactereization od silicon carbide and carbon materials, J. Eur. Ceram. Soc. 35 (2015) 1147–1159.
[4] J. Wade, S. Ghosh, P. Claydon, H. Wu, Contact damage of silicon carbide ceramics with different grain structures measured by Hertzian and Vickers indentation, J. Eur. Ceram. Soc. 35 (2015) 1725–1736.
[5] K.Y. Lim, Y.-W. Kim, K.J. Kim, Mechanical properties of electrically conductive silicon carbide ceramics, Ceram. Int. 40 (2014) 10577–10582.
[6] G. Magnani, A. Brentari, E. Burresi, G. Raiteri, Pressureless sintered silicon carbide with enhanced mechanical properties obtained by the two-step sintering method, Ceram. Int. 40 (2014) 1759–1763.
[7] A. Can, M. Hermann, D.S. McLachlan, I. Sigalas, J. Adler, Densification of liquid phase sintered silicon carbide, J. Eur. Ceram. Soc. 26 (2006) 1707–1713.
[8] M. Hermann, R. Nesher, K. Brandt, S. Hoehn, Micro-segregation in liquid phase sintered silicon carbide ceramics, J. Eur. Ceram. Soc. 30 (2010) 1495–1501.
[9] A. Malinge, A. Coupé, S. Jouannigot, Y.L. Petitcorps, R. Pailler, P. Weisbecker, Pressureles sintered silicon carbide tailored with aluminium nitride sintering agent, J. Eur. Ceram. Soc. 32 (2012) 4419–4426.
[10] A. Noviyanto, D.-H. Yoon, Metal oxide additives for the sintering of silicon carbide: reactivity and densification, Curr. Appl. Phys. 13 (2013) 287–292.
[11] A. Noviyanto, D.-H. Yoon, Rare-earth oxide additives for the sintering of silicon carbide, Diam. Relat. Mater. 38 (2013) 124–130.
[12] E. Sánchez-González, P. Miranda, F. Guiberteau, A. Pajares, Effect of microstructure on the mechanical properties of liquid-phase sintered silicon carbide at pre-creep temperatures, J. Eur. Ceram. Soc. 31 (2011) 1131–1139.
[13] C.-Y. Liu, W.-H. Tuan, S.-C. Chen, Ballistic performance of liquid-phase sintered silicon carbide, Ceram. Int. 39 (2013) 8253–8259.
[14] K. Biswas, G. Rixecker, F. Aldinger, Gas pressure sintering of SiC sintered with rare-earth-(III)-oxides and their mechanical properties, Ceram. Int. 31 (2005) 703–711.
[15] W. Chen, Y. Miyamoto, Fabrication of porous silicon carbide ceramics with high porosity and high strength, J. Eur. Ceram. Soc. 34 (2014) 837–840.
[16] G. Magnani, G. Sico, A. Brentari, P. Fabbri, Solid-state pressureles sintering of silicon carbide below 2000 °C, J. Eur. Ceram. Soc. 34 (2014) 4095–4098.
[17] H. Liang, X. Yao, J. Zhang, X. Liu, Z. Huang, The effect of rare earth oxides on the

pressureles liquid phase sintering of α-SiC, J. Eur. Ceram. Soc. 34 (2014) 2865–2874.
[18] P. Tatarko, S. Lojanová, J. Dusza, P. Sajgalík, Influence of various rare-earth oxide additives on microstructure and mechanical properties of silicon nitride based nanocomposites, Mat. Sci. Eng. A 527 (2010) 4771–4778.
[19] S. Ribeiro, G.C. Ribeiro, M.R. Oliveira, Properties of SiC ceramics sintered vai liquid phase using Al_2O_3+ Y_2O_3, Al_2O_3+Yb_2O_3 and Al_2O_3+Dy_2O_3 as additives: a comparative study, Mater. Res 18 (2015) 525–529.
[20] A. Noviyanto, D.-H. Yoon, Metal oxide additives for the sintering of silicon carbide: Reactivity and densification, Curr. Appl. Phys. 13 (2013) 287–292.
[21] R. Bollina, R.M. German, Heating rate effects on microstructural properties of liquid phase sintered tunsgsten heavy alloys, Int J. Refract Met. Hard Mater. 22 (2004) 117–127.
[22] F. Raether, M.L. Arefin, Kinetic field approach to study liquid phase sintering of ZnO based ceramics, Ceram. Int. 36 (2010) 1429–1437.
[23] F.V. Motta, R.M. Balestra, S. Ribeiro, S.P. Taguchi, Wetting behavior of SiC ceramics: Part II—Y_2O_3/Al_2O_3 and Sm_2O_3/Al_2O_3, Mater. Lett. 58 (2004) 2810–2814.
[24] R.M. Balestra, S. Ribeiro, S.P. Taguchi, F.V. Motta, C. Bormio-Nunes, Wetting behaviour of Y_2O_3/AlN additive on SiC ceramics, J. Eur. Ceram. Soc. 26 (2006) 3881–3886.
[25] S. Ribeiro, S.P. Taguchi, F.V. Motta, R.M. Balestra, The wettability of SiC ceramics by molten E_2O_3(ss)/AlN (E_2O_3(ss)=solid solution of rare earth oxides, Ceram. Int. 33 (2007) 527–530.
[26] J.A. Silva, B.M. Moreschi, G.C.R. Garcia, S. Ribeiro, Wettability of silicon carbide ceramic by Al_2O_3/Dy_2O_3 and Al_2O_3/Yb_2O_3 systems, J. Rare Earth 31 (2013) 634–638.
[27] M. Omori, H. Takei, Preparation of pressureless-sintered SiC–Y_2O_3–Al_2O_3, J. Mater. Sci. 23 (1988) 3744–3749.
[28] B. Desplanques, F. Valdivieso, S. Saunier, Influence of processing parameters on the behaviour of thick bilayers (Cer/Cer) performed by powder processing: Dilatometry without contact, Ceram. Int. 40 (2014) 15215–15225.
[29] A. Karamanov, B. Dzhantov, M. Paganelli, D. Sighinolfi, Glass transition temperature and activation energy of sintering by optical dilatometry, Thermochim. Acta 553 (2013) 1–7.
[30] D. Li, S. Chen, W. Shao, X. Ge, Y. Zhsng, S. Zhang, Densification evolution of TiO_2 ceramics during sintering based on the master sintering curve theory, Mater. Lett. 62 (2008) 849–851.
[31] S.M. Tebcheran, J.A. Varela, Z. Brankovic, G. Brankovic, Sintering kinetcs for SnO_2-based systems constant heating rate, Cerâmica 49 (2003) 99–109.
[32] M.V. Nikolic, V.P. Pavlovic, V.B. Pavlovic, N. Labus, B. Stojanovic, Application on the master sintering curve theory to non-isothermal sintering of $BaTiO_3$ ceramics, Mater. Sci. Forum 494 (2005) 417–422.
[33] J.-G. Li, T. Ikegami, T. Mori, Low temperature processing of dense samarium-doped CeO_2 ceramics: sintering and grain growth behaviors, Acta Mater. 52 (2004) 2221–2228.
[34] K. Rajeswari, S. Padhi, A.R.S. Reddy, R. Johnson, D. Das, Studies on sintering kinetics and correlation with the sinterability of 8Y zirconia ceramics based on the dilatometric shrinkage curves, Ceram. Int. 39 (2013) 4985–4990.
[35] S. Mitra, A.R. Kulkarni, O. Prakash, Densification behavior and two stage master sintering curve in lithium sodium niobate ceramics, Ceram. Int. 39 (2013) S65–S68.
[36] W. Shao, S. Chen, D. Li, H. Cao, S. Zhang, Construction of the master sintering curve for submicron size alpha-Al_2O_3 based on non-isothermal sintering containing lower heating rates only, Mater. Sci.-Pol. 27 (2009) 97–107.
[37] J. Tatami, Y. Suzuki, T. Wakihara, T. Meguro, K. Komeya, Control of shrinkage during sintering of alumina ceramics based on master sintering curve theory, Key Eng. Mater. 317–318 (2006) 11–14.
[38] K. Traore, T.S. Kabre, P. Blanchart, Sintering of clay from Burkina Faso by dilatometry influence of the applied load and the pre-sintering heating rate, Ceram. Int. 27 (2001) 875–882.
[39] H.H. Zhang, Y.L. Xu, B. Wang, X. Zhang, J.F. Yang, K. Niihara, Effects of heating rate on the microstructure and mechanical properties of rapid vacuum sintered translucent alumina, Ceram. Int. 41 (2015) 12499–12503.
[40] G. Agarwal, R.F. Speyer, W.S. Hackenberger, Microstructural development of ZnO using a rate-controlled sintering dilatometer, J. Mater. Res. 11 (1996) 671–679.
[41] M. Mazaheri, A. Simchi, M. Dourandish, F. Golestani-Frad, Master sintering curves of a nanoscale 3Y-TZP powder compacts, Ceram. Int. 35 (2009) 547–554.
[42] R. Caruso, N. Mamana, E. Benavidez, Densification kinetics of ZrO_2-based ceramics using a master sintering curve, J. Alloy. Compd. 495 (2010) 570–573.
[43] J. Banerjee, A. Ray, A. Kumar, S. Banerjee, Studies on sintering kinetics of ThO_2-UO_2 pellets using master sintering curve approach, J. Nucl. Mater. 443 (2013) 467–478.
[44] R.F.K. Gunnewiek, R.H.G.A. Kiminami, Effect of heating rate on microwave sintering of nanocrystalline zinc oxide, Ceram. Int. 40 (2014) 10667–10675.
[45] B. Yavas, F. Sahin, O. Yucel, G. Goller, Effect o particle, heating rate and CNT addition on densification, microstructure and mechanical properties of B4C ceramics, Ceram. Int. 41 (2015) 8936–8944.
[46] J. Marchi, J.C. Bressiani, A.H.A. Bressiani, Densification studies of silicon carbide-based ceramics with ytria, silica and alumina as sintering additives, Mater. Res. 4 (2001) 231–236.
[47] ASTM E-112.